# Resolution limits for electron-beam lithography

by A. N. Broers

This paper discusses resolution limits for electron-beam fabrication. Electron beams have been used to produce structures 1 nm in size and useful devices with minimum features of about 20 nm. In all cases the resolution is set primarily by the range of the electron interaction phenomena that form the structures, and not by the size of the electron beam used to write the patterns. The beam can be as small as 0.5 nm. All useful devices built to date have been fabricated with conventional resist processes; these have an ultimate resolution of about 10 nm. Experimental data for PMMA, the highestresolution electron resist, show that resolution is independent of molecular weight and is therefore not a function of the molecular size. The most promising of the methods offering resolution below 10 nm is the direct sublimation of materials such as AIF<sub>3</sub> and AI<sub>2</sub>O<sub>3</sub>; 1-nm structures have been fabricated, but it has not been possible to convert the structures into useful devices. In addition to the processes which use intermediate patterned layers, there is the possibility of making devices by direct modification of the electrical properties of conductors, semiconductors, or superconductors by means of high-energy

©Copyright 1988 by International Business Machines Corporation. Copying in printed form for private use is permitted without payment of royalty provided that (1) each reproduction is done without alteration and (2) the Journal reference and IBM copyright notice are included on the first page. The title and abstract, but no other portions, of this paper may be copied or distributed royalty free without further permission by computer-based and other information-service systems. Permission to republish any other portion of this paper must be obtained from the Editor.

electron bombardment. In these cases no intermediate fabrication process would be used, and it might be possible to reach dimensions comparable to the beam diameter.

# Introduction

There are several methods for using electron beams to produce structures with dimensions below 100 nm. They include the exposure of conventional and vapor resists, the direct sublimation of materials such as AlF<sub>3</sub> and MgF<sub>2</sub>, the exposure or direct patterning of Langmuir–Blodgett films, and the direct modification of the electrical or chemical properties of conductors, semiconductors, and superconductors. This paper discusses the factors that set the ultimate resolution of electron-beam lithography processes.

Electron-beam lithography techniques produce higher resolution than corresponding ion or X-ray methods because the resolution of electron-beam writing systems is higher. The limits of electron-beam fabrication are therefore the limits of lithography. It should be pointed out, however, that there are means of fabricating structures below 100 nm that avoid lithography altogether by making use of sharp steps on surfaces. The author has discussed these and the alternatives to electron beams in a recent review article [1].

Figure 1 shows the range of sizes encompassed by thinfilm devices. The region of interest in this paper is that below 100 nm. Because optical microscopes can "see" but not resolve 100-nm structures, electron microscopes or scanning tunneling microscopes must be used to inspect the devices.

Structures of 100 nm were first produced with electrons in the early 1960s, but they were not used for any purpose, they were merely examined with an electron microscope [2, 3]. The first useful sub-tenth-micron structures (nanostructures) were fabricated in 1972 [4]. These were aluminum conductors with cross sections of about 60 nm  $\times$  60 nm which were used to measure one-dimensional fluctuation conductivity over a temperature range much larger than had previously been possible. They were fabricated on bulk silicon substrates with PMMA resist and the lift-off process of Hatzakis [5]. Polymethyl methacrylate, PMMA, was first identified as a high-resolution electron resist in 1968 [6]. In 1970, PMMA and lift-off had also been used to produce the first operational electronic devices with dimensions beyond the capability of optical lithography. These were surface acoustic wave devices with dimensions of 0.15  $\mu$ m [7].

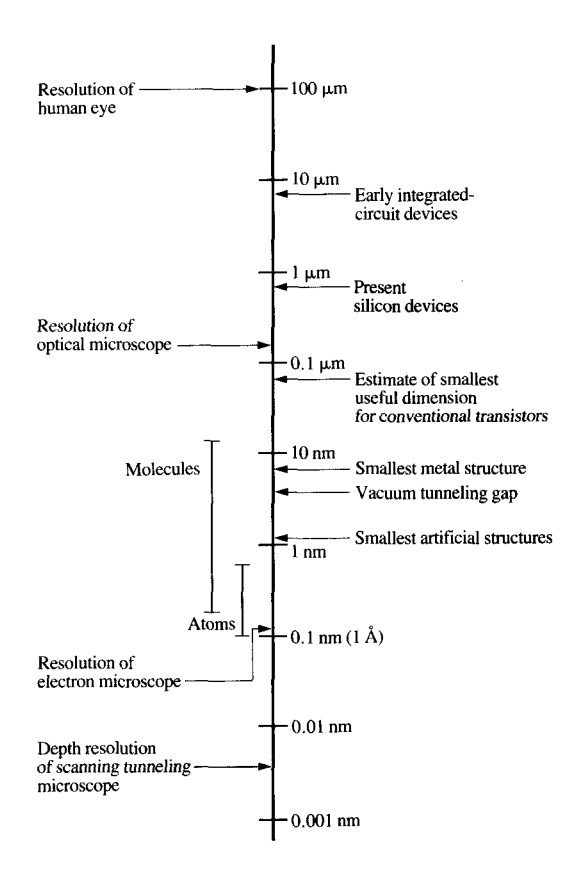
Early nanostructures were also made with vapor or "contamination" resist. This resist, which is described below, was used with ion etching to produce 50-nm-wide metal lines on bulk substrates in the 1960s [3, 8, 9]. In 1976 the same combination was used, together with a thin-membrane substrate, to produce 8-nm metal structures [10] and to make useful devices with dimensions of a few tenths of a nanometer in 1978 [11]. More recently, semiconductor devices with dimensions in the nanostructure region have been fabricated using double-layer PMMA-based resists and lift-off metallization [12, 13].

Structures considerably smaller than 50 nm can be made with electron-beam fabrication, but their "useful" size is frequently limited by imperfections in the thin films from which they are made, and by damage induced in the edges of features by dry etching. These topics are not discussed here. Ultimately it would be preferable to form the devices by selective epitaxial growth, thereby avoiding etching and realizing single-crystal structures.

At present, the major applications for sub-50-nm structures are scientific, and it is not essential that the methods be suitable for mass production, as it is with the related electron-beam methods used to make integrated circuits. The speed of writing and the cost of equipment are therefore not as important and are not discussed here.

# Electron-optical resolution beam size

In the absence of the need for high beam current and large scanned area, the minimum diameter of an electron probe is set by the axial aberrations of the final probe-forming lens and diffraction. The operating aperture for the lens is chosen as a compromise between the conflicting requirements of these two deleterious effects. Spherical aberration is the dominant aberration, and gives rise to a "disk of confusion" with a diameter that increases with the third power of the beam aperture. Diffraction causes an Airy disk pattern whose diameter decreases linearly as the beam aperture increases. The optimum choice of beam aperture yields a minimum beam diameter of  $kC_s^{1/4} \lambda^{3/4}$ , where  $C_s$  is the spherical aberration coefficient of the lens and  $\lambda$  is the electron wavelength; k is a constant that depends upon the beam



# 37. T. T. W.

Size scale for microstructures and microscopy.

diameter. It is about 0.9 when 80% of the beam current is contained within the beam diameter. For the shortest-focal-length electron lenses,  $C_s$  is about 0.5 mm when focusing 100-keV electrons (wavelength of 0.004 nm), and then the minimum beam diameter is 0.37 nm.

The degree to which the beam diameter approaches a theoretical minimum depends on the brightness of the electron source and the beam current. In theory, the minimum value is only reached for infinite brightness or zero beam current. In practice, currents up to about  $10^{-10}$  A are available with field-emission cathodes and up to  $10^{-12}$  A with thermal cathodes before the beam grows 20% above the theoretical minimum. Figure 2 shows the relationship between beam diameter and beam current for the lanthanum-hexaboride-cathode electron-beam system used to fabricate the nanostructures described in this paper. It is assumed that the optimum beam aperture is used in all cases. The theoretical minimum beam diameter for 50 kV is 0.56 nm.

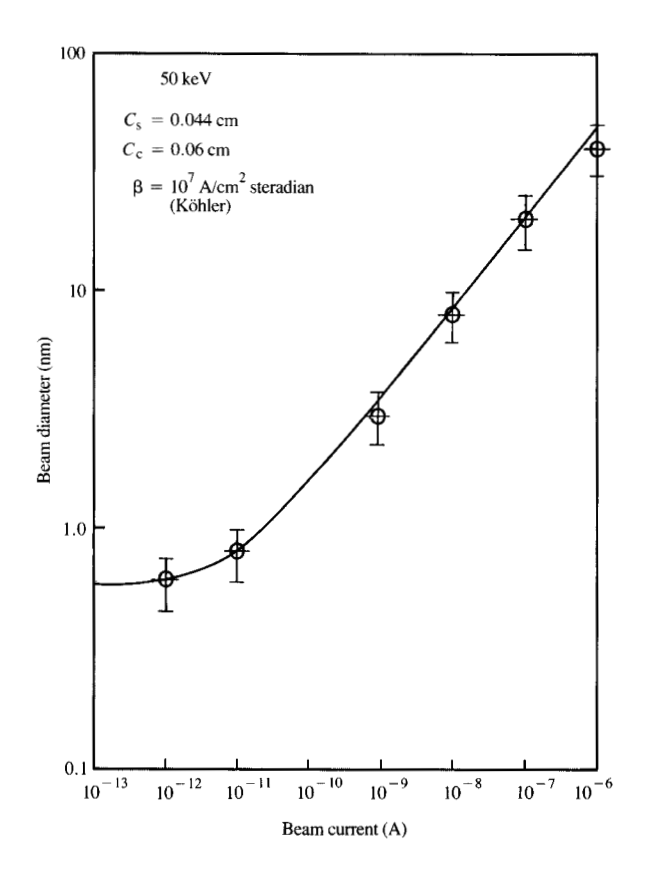


# Figure 2

Beam size versus current for the electron-beam system used to fabricate the nanostructures shown in this paper. The method used to make the theoretical estimate of beam diameter and current is described in [16].

Currents of about a picoampere are adequate for resist exposure when the minimum feature size is about 10 nm. For example, with a resist sensitivity of  $0.5 \times 10^{-4}$  C/cm<sup>2</sup>, only 30 electrons are required to expose a single 1-nm pixel, and the beam-incrementing rate is 200 kHz for a beam current of  $10^{-12}$  A. With the lenses used for nanolithography, the deflection coil is placed in the pole-piece bore, and 200 kHz is close to the maximum rate attainable before the onset of pattern distortion due to eddy currents induced in the iron pole-pieces of the final lens. It is not possible to use ferrite pole-pieces, as is done in high-speed semiconductor lithography systems, because ferrites cannot sustain the much higher magnetic excitation of the short-focal-length nanolithography lens. The ferrite pole-pieces are electrically insulating and do not sustain eddy currents.

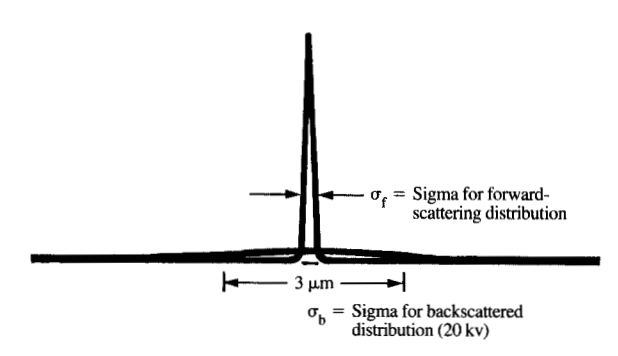
# Electron-beam exposure of conventional resists

Several factors other than the size of the electron beam determine the extent of the exposed volume in a layer of

conventional resist. For integrated-circuit lithography, where at present relatively low accelerating voltages and thick resists are used, electron scattering is the most important factor. For nanolithography, where higher accelerating voltages and thinner resists are used, secondary-electron generation is the most important factor, and the effects of scattering are unimportant. We believe that it is the delocalization of secondary-electron generation, together with the subsequent straggling of the secondary electrons into the resist, that sets the ultimate resolution limit for nanolithography.

# ◆ Electron scattering

Figure 3 shows qualitatively the mechanisms of electron scattering. The resist is exposed by both the incident electrons and the electrons scattered back from the substrate.



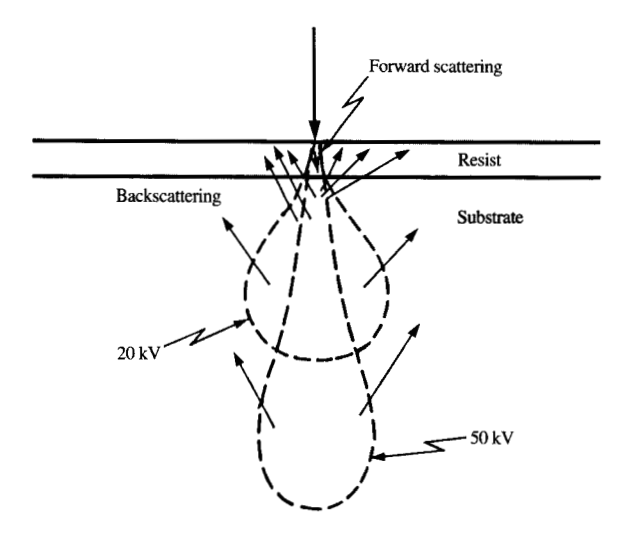


# Figure 6

Electron scattering in electron resist exposure. The curves at the top of the figure show the exposure distributions due to the incident and backscattered electrons.

Lateral scattering of the primary electrons as they penetrate the resist gives rise to the narrower of the distributions, the "forward-scattering" distribution. Backward scattering of electrons from the substrate gives rise to the broader distribution, the "backscattering" distribution. The distributions are generally assumed to be Gaussian, and they are assigned sigma values:  $\sigma_f$  for forward scattering and  $\sigma_b$  for backscattering. The overall exposure distribution is given by the proximity function  $F_p(r)$ , where

$$F_{\rm p}(r) = k[\exp{-(r/\sigma_{\rm f})^2} + \eta(\sigma_{\rm f}/\sigma_{\rm b})^2 \exp{-(r/\sigma_{\rm b})^2}],$$
 (1)

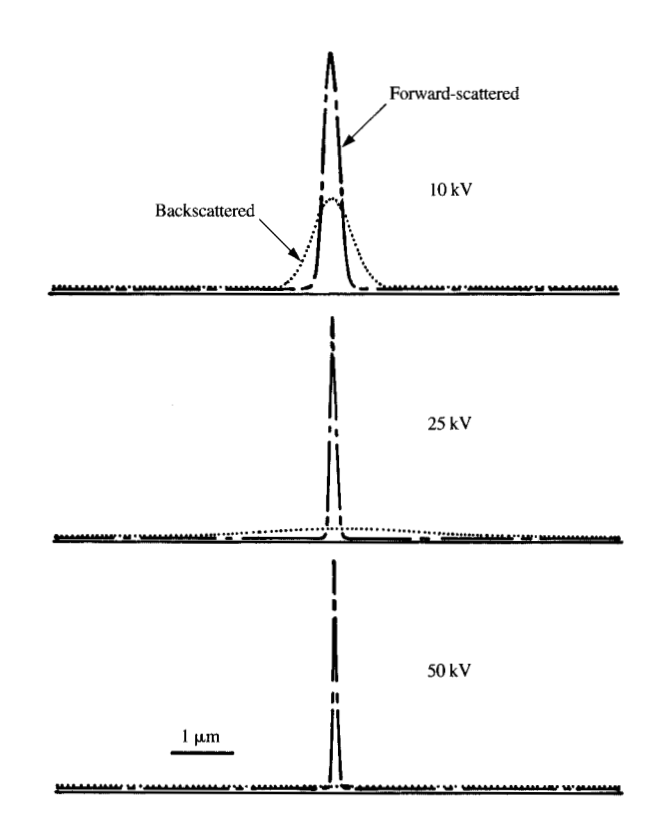
and r is the radial distance from the center of the exposure distribution,  $\eta$  is the ratio between the exposure due to the backscattered electrons and the incident electrons, and k is a normalizing constant.

Several workers have used Monte Carlo methods (e.g., Kyser and Murata [14]) to model electron scattering for resist exposure; their results are in broad agreement with experiment and support the assumption that the distributions are Gaussian.

Figure 4 shows approximate distributions for the electron-beam exposure of a 1- $\mu$ m-thick resist layer on a silicon substrate at incident electron energies of 10 kV, 25 kV, and 50 kV. It can be seen that the width of the forward-scattering distribution is reduced as the electron energy increases. Although it is not shown, it is obvious that the forward scattering width is also reduced for thinner resist layers. The rates of reduction in each case are such that forward scattering becomes negligible for the combination of 50 keV and resist thicknesses below about 0.1  $\mu$ m [15]. Nanofabrication methods operate in this regime and forward scattering can be ignored.

Figure 4 also indicates that the width and intensity of the backscattered distribution depend upon the incident electron energy. The greater the incident energy, the larger the disk from which electrons are backscattered from the substrate. The total exposure due to the backscattered electrons is very approximately independent of beam energy and is equal to the exposure due to the incident electrons. As the energy of the incident electrons increases, the backscattered exposure spreads more and more, until by the time the electron energy reaches 50 keV, the diameter is so large,  $>5 \mu m$ , that the backscattered electrons only produce a background "fog." This fog builds up for dense patterns, and in extreme cases can limit resolution by reducing contrast. Elementary considerations lead to the conclusion that the maximum contrast for a pattern of equal lines and spaces is 0.5, assuming equal exposure by incident and backscattered electrons.

For small isolated features, backscattering has a negligible effect on contrast or resolution. For nanolithography the only significant effect of backscattering is that it reduces contrast for very dense patterns, and even this disadvantage can be avoided by using membrane substrates.



# a foldtig ag

Exposure distributions for a 1- $\mu$ m-thick resist layer on a silicon substrate for 10 kV ( $\sigma_f=0.3~\mu m,\,\sigma_b=0.8~\mu m,\,\eta=1$ ), 25 kV ( $\sigma_f=0.12~\mu m,\,\sigma_b=3~\mu m,\,\eta=0.86$ ), and 50 kV ( $\sigma_f=0.07~\mu m,\,\sigma_b=8~\mu m,\,\eta=0.5$ ) electrons. The electron-scattering parameters  $\sigma_f,\,\sigma_b$ , and  $\eta$  are defined in the text.

# Secondary electrons

Electrons with energies above about 5 eV can break or make chemical bonds and thereby expose resist. This means that the free, low-energy, secondary electrons produced by inelastic interactions between high-energy electrons (either scattered or primary) and the resist atoms are important in resist exposure. These low-energy secondaries, which typically have energies up to about 20 eV, can be excited remotely from the high-energy incident electron beam and may straggle further into the resist before their energy is dissipated. As already mentioned, we believe that these secondary electrons set the  $\approx$ 10-nm resolution limit measured by the method described in the section on measurement of exposure distribution in resists.

A similar process limits the resolution of the best secondary-electron-surface scanning electron microscopes

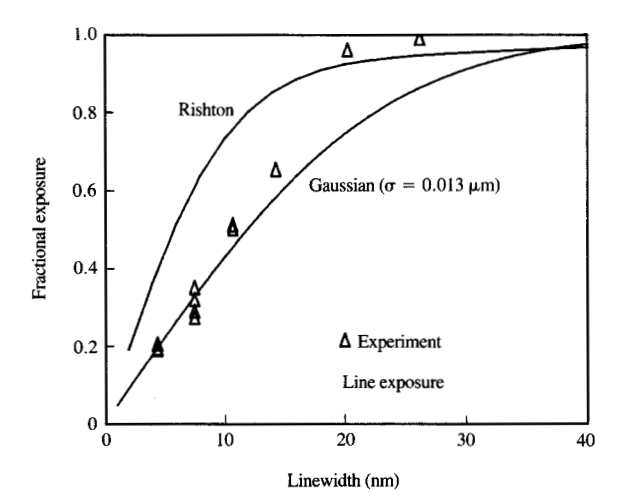


# Figure 5

Fractional exposure (ratio of exposure received at the center of lines compared to the exposure received at the center of a large shape) for PMMA exposed with 50-kV electrons. Experimental results suggest that beyond about 10 nm the interaction range of the electrons falls off more steeply than a Gaussian distribution.

(SEMs). In the SEM, the area from which secondary electrons are emitted is also larger than the electron beam. There are many factors determining the diameter over which secondaries are excited, and the diameter is difficult to measure accurately, but estimates made from the "sharpness" of SEM images [16] suggest that it is 2–5 nm for metals. This leads to a resolution limit of about 10 nm, which is similar to the e-beam lithography limit and supports the argument that it is the secondary-electron delocalization that imposes this limit. However, the support is by no means rigorous because the range of the secondary interactions may not be the same in resist as it is in the metals.

The conclusion that the delocalization of the secondary-electron exposure gives rise to the 10-nm limit is not supported by the work of Rishton [17]. Rishton's data suggest that the exposure distribution due to secondaries is narrower than 10 nm. Rishton combined direct measurements of the low-energy electron range with the electron energy-loss data of Ritsko [18]. Figure 5 shows the exposure received at the center of lines as a function of their width for Rishton's distribution, experimental data described below for PMMA resist, and the Gaussian distribution suggested by the author as an adequate fit to the experimental data. The discrepancy between the experimental width and the data of Rishton could be a phenomenon related to the size of the PMMA molecules or

the extent of the "chemical" development process. These factors are discussed in the next section.

The parameter plotted on the ordinate of Figure 5, fractional exposure, is defined as the ratio of the exposure dose at the center of an infinitely long rectangle of the linewidth shown in Figure 5, to the exposure received at the center of an infinitely large shape. For rectangles narrower than the width of the exposure distribution, the dose at the center of the rectangle falls off at a rate determined by the shape of the exposure distribution.

The situation is made more complex by the creation of secondaries at the interface between the resist and the substrate. For substrate materials with high secondary-electron coefficients, such as gold, there may be more secondaries created at the interface than in the resist. Measurements of the ultimate resolution of resist exposure have not been made as a function of substrate, so this effect cannot be quantitatively evaluated. The interface secondaries give rise to an undercut resist profile which limits the resolution, or at least the minimum separation between features, but may be useful for lift-off processing.

# Molecular weight and chemical amplification

The size of the resist molecules and the extent of the chemical reaction that results from the exposure process are factors which can potentially affect resolution. While there are cases where the "range" of the chemical interaction sets the minimum feature size, as for example with silver halide emulsions where exposure triggers the growth of crystals that may be larger than the exposed area, there is no evidence that this is the case for the highest-resolution resists such as PMMA, where there is no such "chemical amplification." In other words, the chemical change is restricted to the point at which the electron breaks or makes a chemical bond and does not trigger an extended reaction such as the crystal growth observed in silver halide emulsions. In fact, there is little indication of degradation even when chemical amplification is present, as in the case of the poly(p-tbutyloxycarbonyloxystyrene (t-BOC) resist described by Umbach et al. in this issue of the IBM Journal of Research and Development. The resist exposure distribution function has been measured for t-BOC and it turns out to be about the same as that for PMMA. The experimental measurements with PMMA and t-BOC lead to the conclusion that neither molecular weight nor chemical amplification is important in determining the ultimate resolution.

• Measurement of exposure distribution in resists

It is difficult to measure the ultimate resolution of electron resists because resist test patterns become distorted by irradiation in the electron microscopes needed to make linewidth measurements. This difficulty led to the development of a method that determines effective exposure

distribution without the need to measure linewidth [15]. All that is required is a knowledge of the nominal "written" linewidth, and a determination of which lines are completely exposed at each exposure dose. The exposure distribution measured in this way can be used to determine resolution in the same way the Airy distribution is used to determine the resolution of a diffraction-limited optical microscope.

A test pattern of the type used to determine the exposure distribution is shown in Figure 6. The pattern was written in a 60-nm-thick layer of PMMA with a 50-kV electron beam with a diameter of 0.5 nm. The minimum "written" linewidth (4 nm) was about three times smaller than the half-width of the distribution, and the largest linewidth was about 10 times greater than the half-width. For each experiment, the pattern was repeated at about 10 different exposure doses. The lightest dose was less than that needed to open up the largest shapes. The heaviest dose was high enough to ensure that the resist develops through to the substrate in the site of the narrowest line. At a critical intermediate dose, the large shapes barely develop through the substrate, and shapes that are smaller than the exposure distribution do not receive enough exposure to develop completely. As the exposure dose is increased from this intermediate value, smaller shapes develop and the exposure distribution can be derived from the additional dose needed for each aperture size. The resist pattern shown in Figure 6 was exposed at a dose slightly greater than that needed to open up the largest shapes.

Assuming that the exposure distribution is Gaussian, and that the lines are equivalent to infinitely long rectangles, the exposure dose  $Q_{\rm w}$  (C/cm²) received at the center of a line is given by  $Q_{\rm w}=Q_0{\rm erf}(W/2\sigma)$  (C/cm²) where  $Q_0$  (C/cm²) is the exposure dose in the center of the infinitely large shape, and  $\sigma$  is the standard deviation of the distribution.  $Q_{\rm w}$  is measured for each linewidth by determining the dose at which the line first develops through to the substrate. As the exposure increases, narrower and narrower lines develop through to the substrate. The exposure distribution is calculated from  $Q_{\rm w}$  versus linewidth data of the type shown in Figure 7.

Figure 7 also shows data for PMMA of different molecular weights and indicates that the width of the exposure distribution does not depend upon molecular weight. These experiments, which show an exposure distribution half-width of 10 nm to 20 nm, are reported here for the first time. They were carried out in collaboration with C. G. Willson, C. Umbach, R. Koch, and R. Laibowitz of the IBM T. J. Watson Research Center.

# • Exposure versus feature size for thin-film and bulk substrates

In order to come up with an overall estimate for the resolution of electron-beam exposure of PMMA, data for a thin substrate and thin resist (60 nm) are shown in Figure 8

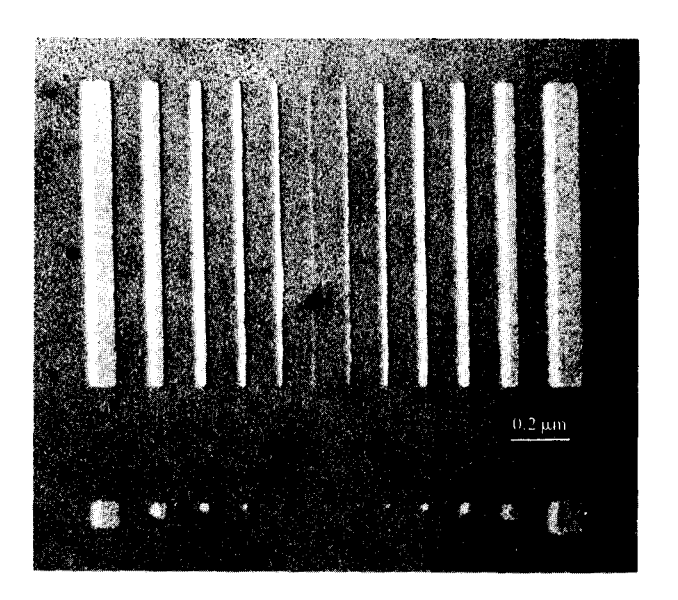


# Figure 6

One of a series of test patterns used to measure the resolution of electron resist [14]. The 60-nm-thick PMMA resist layer is supported on a 60-nm-thick  $\mathrm{Si}_3\mathrm{N}_4$  membrane; the pattern has been exposed with a 0.5-nm-diameter 50-kV electron beam. The sample has been shadowed at 45° with AuPd in order to highlight the structure and to reveal the resist thickness. This particular exposure is made at a slightly larger dose than is needed to open up the largest shapes in the pattern.

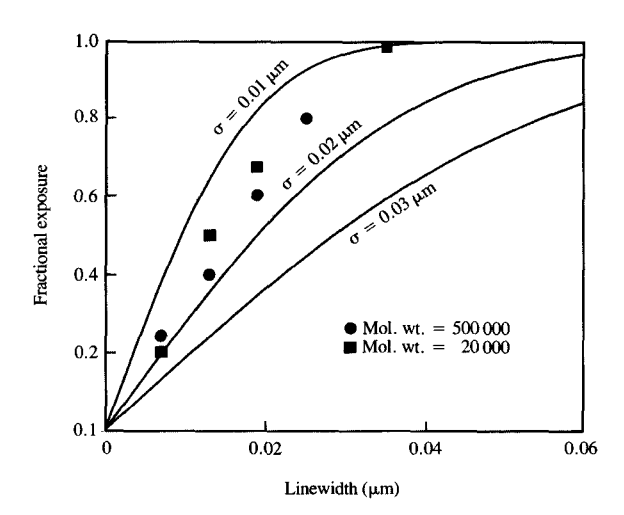
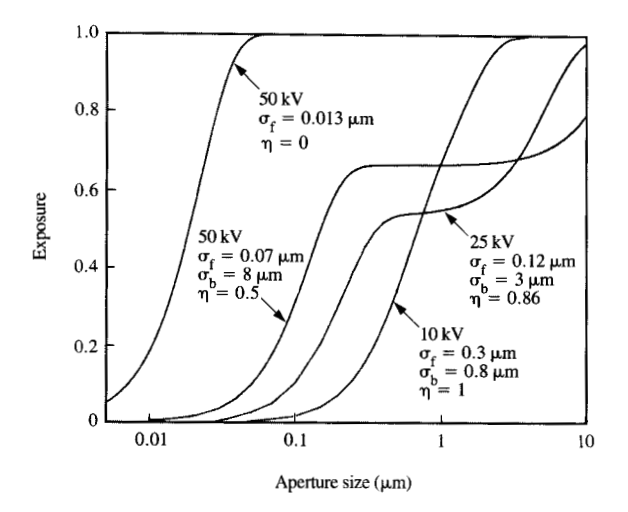


# Figure 7

Fractional exposure data for PMMA of 20 000 and 500 000 molecular weight. The difference between the data for the different molecular weights is negligible, suggesting that there is no dependence on the molecular weight of the sample. These experiments were carried out in collaboration with C. G. Willson, C. Umbach, R. Koch, and R. Laibowitz of the IBM Thomas J. Watson Research Center.



Normalized aperture exposure (ratio of the exposure received at the center of a square aperture of a given size to the nominal background exposure) for 10-kV, 25-kV, and 50-kV electron exposure of a 1- $\mu$ m-thick PMMA resist layer on a bulk silicon substrate. The proximity function given in Figure 3 is used to make these estimates. The case for thin resist (<0.25  $\mu$ m) on a thin membrane (such as that shown in Figure 9) is also included. In this instance forward scattering and backscattering are assumed to be insignificant.

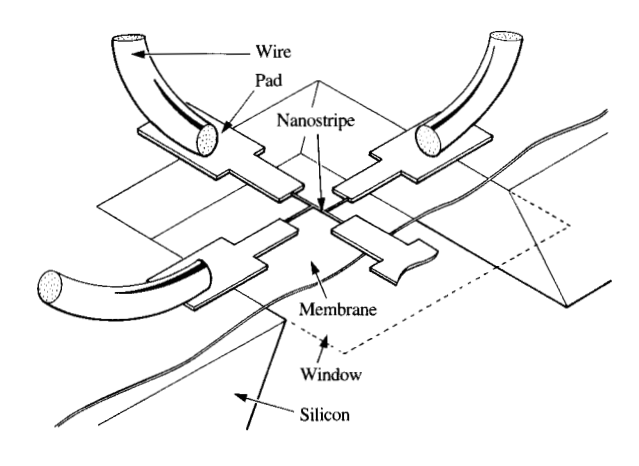


# Figure 9

Diagrammatic view of window substrate that allows contact to be made to devices fabricated on fragile membrane [18, 19].  $\mathrm{Si_3N_4}$  membrane is typically 60 nm thick. A major advantage of the substrate is that samples can be viewed with transmission electron microscopy. Backscattered electrons are also reduced to negligible numbers, so the contrast is better than for exposure on bulk substrates.

together with data for a bulk silicon substrate and relatively thick (1 µm) resist. The different cases can be identified by the scattering parameters ( $\sigma_f$ ,  $\sigma_b$ , and  $\eta$ ) shown in the figure. For example,  $\eta = 0$  (zero backscattering) for the thinmembrane case on the left of the figure. The three other conditions are for the bulk silicon substrate. Figure 8 shows how the exposure at the center of the square shapes (apertures) varies with the size of the square. The exposure is normalized so that the exposure at the center of an initially large square is unity. These data model the most difficult situation in practical lithography, that of writing patterns containing both large and small shapes. For example, at 10 kV a 1-μm square will only receive a normalized exposure of 0.6, while large shapes (greater than about 4  $\mu$ m) will receive an exposure of 1. The development process must therefore tolerate a 40% variation in dose if the 1- $\mu$ m and the 4- $\mu$ m shapes are to develop to their correct sizes.

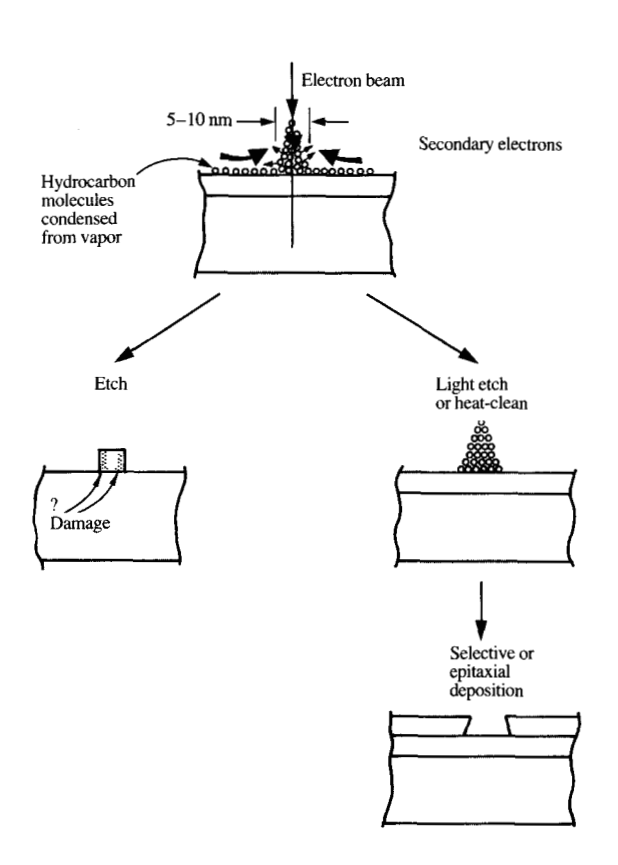
The forward-scattering and backscattering exposure distributions are assumed to be Gaussian, and the overall exposure is that given by Equation (1). The forward-scattering sigmas are those obtained in a recent set of experiments in which the exposure distributions in 1- $\mu$ m-thick PMMA layers were measured in a manner similar to that described above for the measurement of ultimate resolution. The minimum feature size obtainable for each of the cases in Figure 8 can be estimated to be that at which the exposure has fallen to about 0.5: that is, 0.02  $\mu$ m for the 50-kV, thin-substrate, thin resist case, and 0.13  $\mu$ m, 0.36  $\mu$ m, and 0.65  $\mu$ m for the 50, 25, and 10 kV, silicon-substrate, 1- $\mu$ m-thick resist cases.

# Thin-membrane substrate for nanolithography

The measurements of resist resolution just described were made on the thin-film substrate shown in **Figure 9**, which was developed and patented for the fabrication of sub-tenth-micron structures [19, 20]. The principal attribute of the substrate is that it allows samples to be examined with a resolution of about 0.1 nm in transmission electron microscopes, scanning or projection. The secondary-electron scanning electron microscope, which is generally used for the examination of microstructures, is limited in resolution by the range of the secondary electrons in the same way the resolution of resist exposure is limited. It is therefore not possible to use the SEM for studying resist resolution limits.

The thin-membrane substrate also greatly reduces the number of backscattered electrons from the substrate and hence improves contrast. Its final attribute is that it is possible to make electrical contact to structures fabricated upon thin membranes. This is done by the contact pads that extend out from the bulk area as shown in Figure 9.

Thin membranes of a variety of materials have been made, and it is possible, for example with silicon or GaAs membranes, to fabricate devices using the membrane as part of the device.





Vapor resist (contamination) method for producing nanostructures.

# Electron exposure of vapor resists—contamination lithography

An alternative to spinning a liquid resist onto the sample is to condense vapor onto the surface. This process occurs unavoidably in vacuum systems pumped with untrapped oil diffusion pumps. The condensed hydrocarbon vapors found in these vacuum systems form a negative electron resist which acts as a satisfactory mask for ion etching. As already mentioned, this contamination resist process was developed in the early 1960s and has been used to make a variety of small devices.

Contamination resist is formed when the electron beam "cracks" the thin layer of hydrocarbons at the sample surface. As this process continues, a cone of resist builds up at the point of impact of the electron beam, as shown diagrammatically in Figure 10. The rate of buildup can be increased by increasing the partial pressure of hydrocarbons in the immediate vicinity of the sample with a local source of vapor.

Typically, a dose of 0.1-1 C/cm<sup>2</sup> is required to produce an adequate buildup of "exposed" vapor to protect 100-nm-

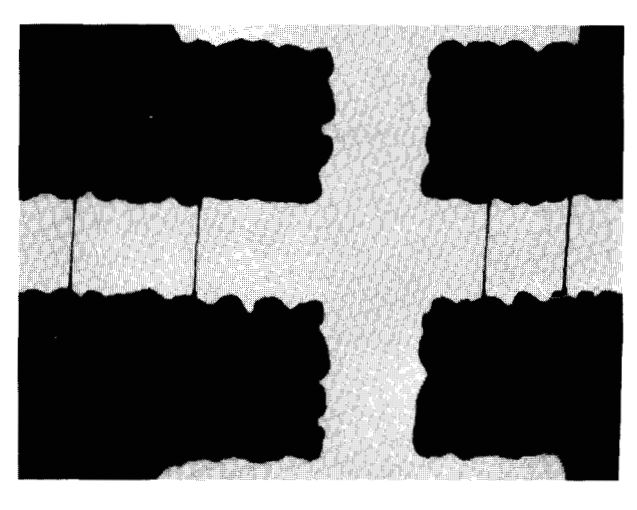


Figure 11

Microbridge SQUIDs fabricated with contamination resist electron-beam lithography [23].

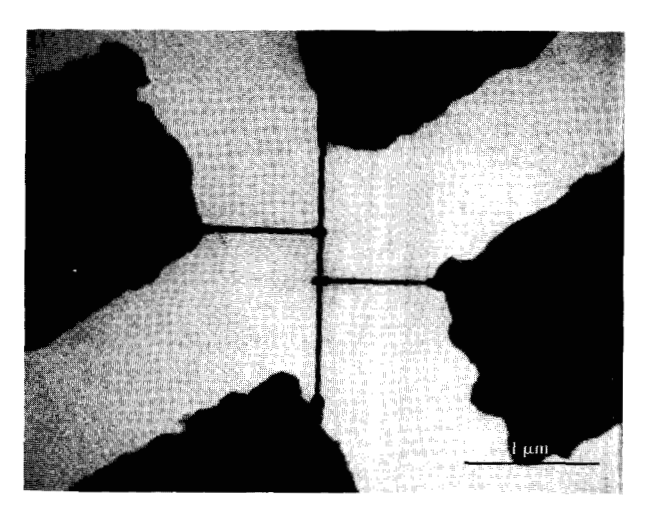
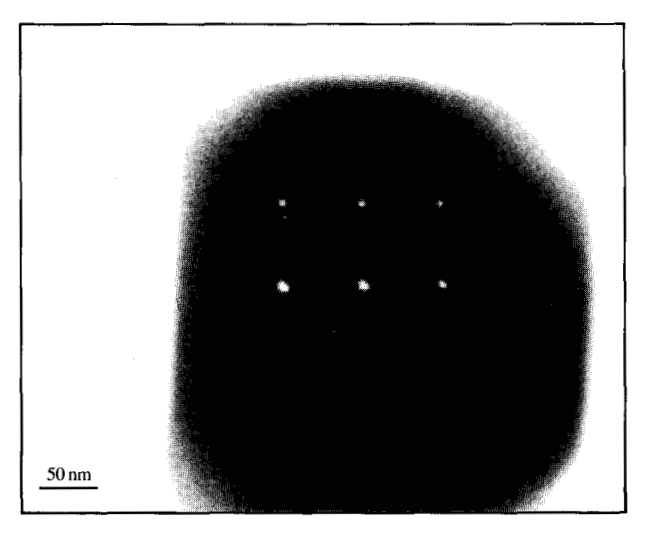


Figure 12

Niobium wires 25 nm wide in a four-terminal configuration used for exploring localization effects [22].

thick metal layers (e.g., gold and niobium) from ion etching. This high dose makes it difficult to fabricate large-area devices in a reasonable time, but has the advantage that the sample can be microscopically examined before and after exposure without significant resist buildup. Transmission microscopy can be used to position the beam with respect to contact pads or other device layers, and to examine the resist pattern after it has been formed. The buildup of resist can also be accurately monitored by observing the decay in the transmitted signal.

It is possible to remove the layer of hydrocarbons and thereby stop the buildup of contamination by heating the



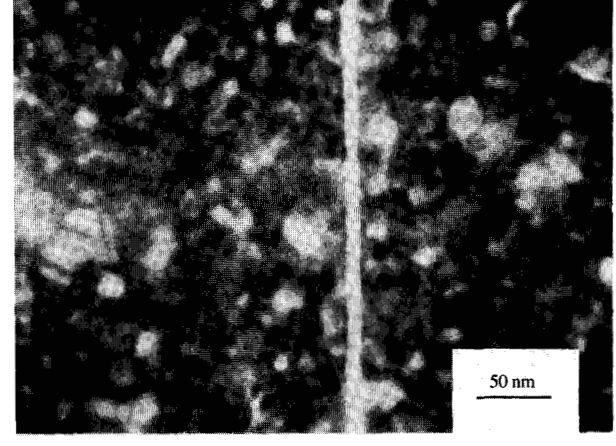


# Figure 13

Holes 5 nm in diameter drilled in 0.25- $\mu$ m-thick NaC1 crystal with 1-nm-diameter electron beam [26].

Figure 14

A 10-nm-wide slot ion-milled in a 20-nm-thick gold film using directly patterned MgF<sub>2</sub> as a mask.

sample to about 100°C. This can be done, for example, with a high-intensity lamp. After the hydrocarbons have been removed, the sample can be examined without further buildup of resist, provided of course that the partial pressure of hydrocarbons is low enough to prevent the formation of a new layer of hydrocarbons. This technique also opens up the possibility for *in situ* fabrication sequences where the vapors which form the resist are selectively introduced when the resist pattern is to be formed, and then removed before the next thin-film deposition step.

A variety of devices have been fabricated with the combination of contamination resist and ion etching, including microbridges [21], SQUIDs (Superconducting Quantum Interference Devices) [22], as shown in Figure 11, fine wires for exploring localization effects [23], as shown in Figure 12, and rings for demonstrating aspects of the Aharonov–Bohm effect [24]. Buckley et al. [25] have produced high-resolution X-ray zone-plate lenses with contamination lithography.

# Sub-10-nm structure fabrication

# • Direct sublimation

To avoid the 10-nm limit encountered with conventional electron resists such as PMMA, it is necessary to find an image-forming process that is activated only by the high-energy primary electrons, and not by the low-energy secondaries.

One process which appears to behave in this manner is the direct sublimation under electron bombardment of a variety

of materials, including NaCl, MgF<sub>2</sub>, AlF<sub>3</sub>, LiF, and Al<sub>2</sub>O<sub>3</sub>. The high resolution of this process was discovered in an experiment proposed by J. W. Matthews that produced the 5-nm-diameter holes shown in Figure 13. The holes were formed in a NaCl crystal by a 1-nm-diameter 50-kV electron beam [26, 27]. The crystal was 0.25  $\mu$ m thick, the convergence half-angle of the beam was 10<sup>-2</sup> radian, and, assuming that the beam was focused on one face of the crystal, the beam would have formed a cone-shaped hole, with the base of the cone being about 5 nm in diameter. This would explain the difference between the apparent size of the hole and the beam diameter, and suggest that the resolution of the process was better than 5 nm. Further experiments demonstrated that it was possible to use a patterned MgF, film to mask a gold film from ion milling and to produce slots 10 nm wide in a 20-nm-thick gold film (see Figure 14). In general, however, the films did not stand up well to a variety of dry or wet etching techniques, and the exposure doses needed were very heavy (0.1 C/cm<sup>2</sup>).

Isaacson and Muray [28] confirmed that resolution below 0.5 nm is possible with direct sublimation by writing structures about 1.5 nm in size in thin NaCl and AlF<sub>3</sub> films. Kratschmer and Isaacson [29] used patterned AlF<sub>3</sub> films to mask a silicon nitride film against dry etching, but the smallest structures produced in the nitride were only about 20 nm in size.

Mochel et al. discovered that the sublimation process works with Al<sub>2</sub>O<sub>3</sub>, and produced holes 1 nm in diameter [30]. Both Mochel et al. and Isaacson et al. have used EELS (Electron Energy Loss Spectroscopy) to analyze the process,

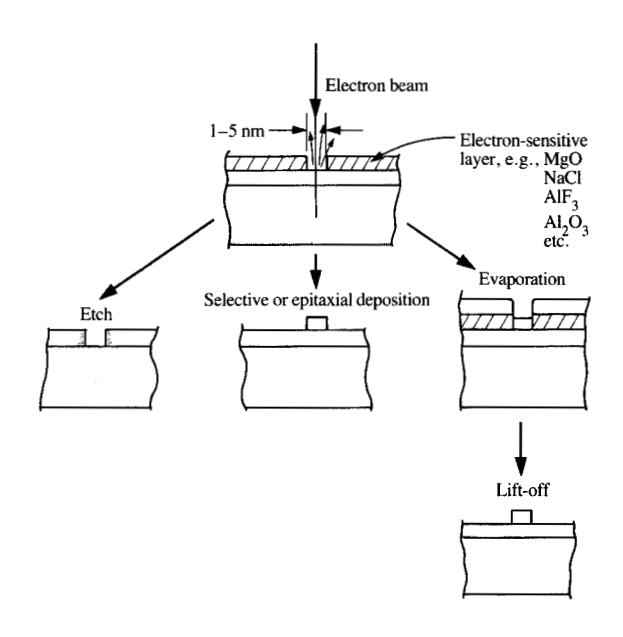
and have shown that a metal-rich deposit remains after the sublimation process. The details of the sublimation mechanism remain unclear, and this process has not as yet produced devices of practical importance. Some of the ways in which device structures might be fabricated with direct-sublimation lithography are shown in **Figure 15**.

• Exposure of multilayer Langmuir-Blodgett films Lines can be written in multilayer Langmuir-Blodgett films (see Figure 16) with much lower dosages ( $\approx 10^{-4} \text{ C/cm}^2$ ) than are required for direct sublimation processes described in the previous section [31]. Minimum linewidths may be smaller than 10 nm, but it is difficult to confirm this because the films become rapidly exposed by the microscope beam. The lines shown in Figure 16 are about 10 nm wide as viewed with bright-field scanning transmission electron microscopy. The lines were shown to be slots by low-angle AuPd shadowing of the samples. We were not successful in using Langmuir-Blodgett stacks of the type shown in Figure 16 as masks for standard dry or wet etching processes, so, as with the direct sublimation methods, we assume that the process will not be useful until complementary structureforming methods are found.

# • Radiation damage lithography

It may be possible to fabricate structures smaller than the electron-resist interaction range by means of processes which use electrons whose energy is great enough to cause radiation damage in the sample. For crystalline materials such as silicon this requires an energy above ~150 keV. Several potential methods for converting the damaged areas into structures are shown in Figure 17. The damage may enhance or retard the etch rate of the material for dry or wet etch processes, it may locally change other properties such as the critical temperature of superconductors, or it may locally affect the integrity of epitaxial films grown on the substrate. In the case of epitaxial films, damaged areas may etch at a different rate than defect-free areas, or may exhibit different electrical properties (conductivity, etc.). An example of the latter might be that regions of a superconducting film deposited on damaged areas of a single-crystal substrate would exhibit normal conductivity and therefore act as weak links between the superconducting regions grown on the undamaged areas.

Electrons with an energy of less than half the damage threshold energy could be used for radiation-damage lithography, so that only a single damage event would be created by each electron. The damage should then be localized within the beam diameter, which could be as small as 0.3 nm. Jones et al. have carried out some preliminary experiments which have confirmed the mechanism of this process [32].



# Figure

Possible methods for fabricating structures with direct-sublimation electron-beam lithography. Selective deposition methods could include electroplating.

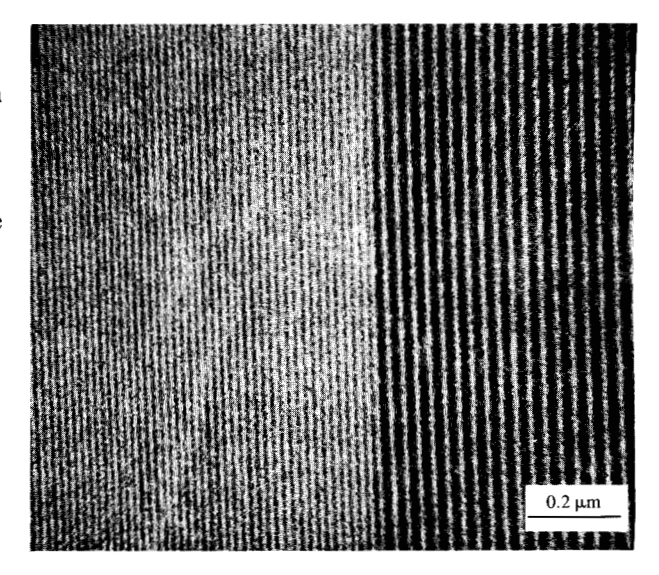


# Figure 16

Bright-field STEM micrograph of lines written in a stack of manganese-stearate Langmuir-Blodgett films.

# Summary

Several methods can be used to fabricate thin-film devices with electron beams. Exposure of conventional resists is the most generally applicable method and can produce useful

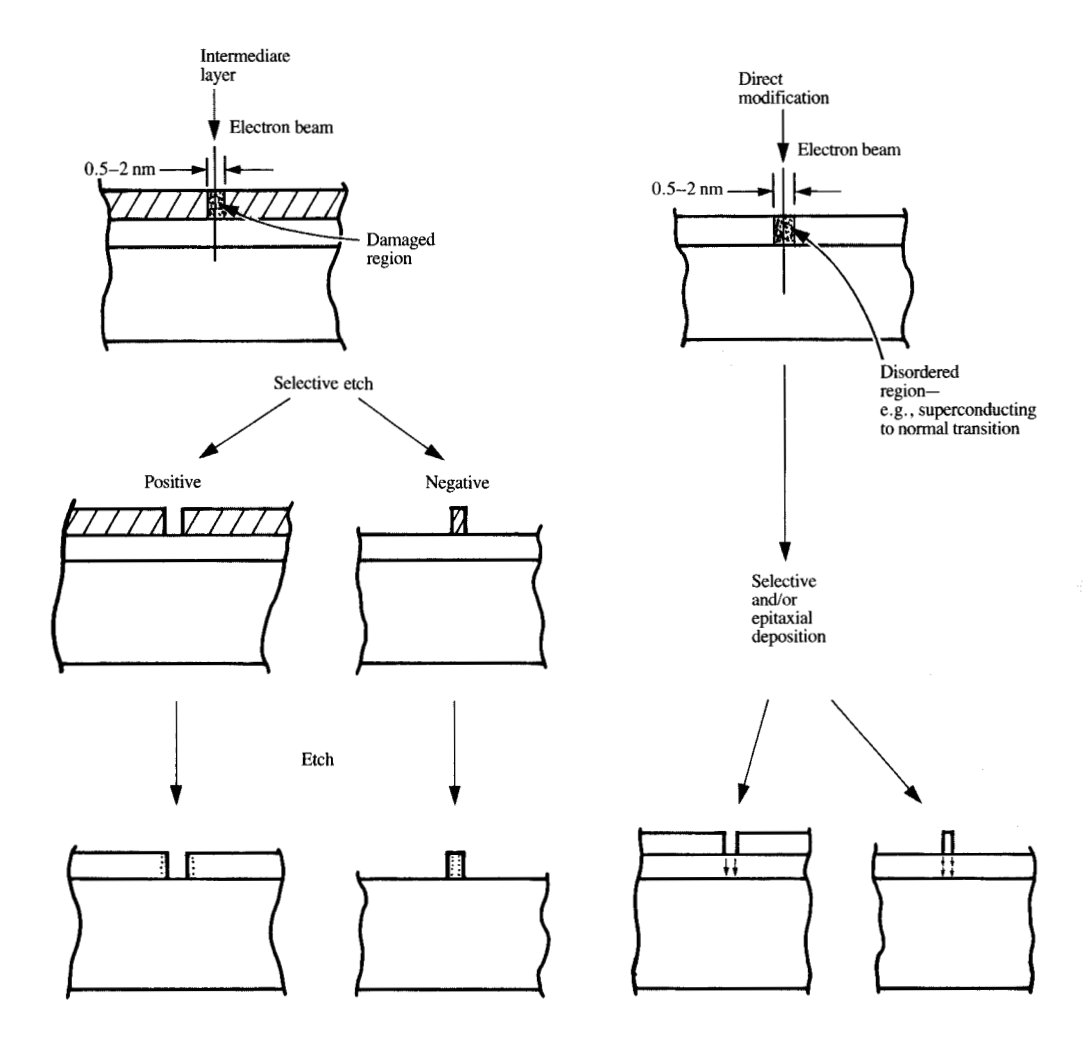


Figure 17

Possible methods for using electron-beam-induced radiation-damage lithography to fabricate structures.

structures with dimensions of about 10 nm. For dense patterns, the minimum features are about twice this size. The 10-nm limit is thought to be due to the delocalization of the exposure by secondary electrons. A similar limit is encountered with vapor or contamination resists, although it may be possible in this case to produce slightly smaller isolated features; e.g., 8-nm conductors have been made. Contamination resist is not useful for large-area structures unless a continuous source of vapor is provided, but has proven valuable for simple nanostructure devices because it allows pattern registration and resist buildup to be monitored *in situ*.

Direct sublimation of the alkali halides and other materials leads to structures that more closely approach the minimum electron-beam size of 0.5 nm, but it has not yet proven possible to convert these structures into useful devices.

The direct modification of the electrical properties of materials with electron beams also offers the potential for devices with elements about the same size as the minimum beam diameter of 0.5 nm, but only a few preliminary experiments have explored this idea.

# **Acknowledgments**

The author acknowledges with thanks his colleagues at IBM Research, with whom he was privileged to work in establishing the resolution limits of electron-beam lithography.

512

# References

- A. N. Broers, "Limits of Thin Film Microfabrication," Proc. Roy. Soc. Lond., to be published, 1988.
- G. Mollenstedt and R. Speidel, "Elektronoptischer Mikroschreiber unter Elektronenmikroskopischer Arbeitskontrolle," Phys. Blatter 16, 192 (1960).
- A. N. Broers, "Combined Electron and Ion Beam Processes for Microelectronics," *Electronics and Reliability*, Vol. 4, Pergamon Press, U.K., 1965, pp. 103-104.
- A. F. Mayadas and R. B. Laibowitz, "One-Dimensional Superconductors," Phys. Rev. Lett. 28, 156-158 (1972).
- M. Hatzakis, "Electron Resists for Microcircuit and Mask Production," J. Electrochem. Soc. 116, 1033 (1969).
- I. Haller, M. Hatzakis, and R. Srinivasan, "High-Resolution Positive Resists for Electron-Beam Exposure," IBM J. Res. Develop. 12, 251 (1968).
- E. G. Lean and A. N. Broers, "Microwave Surface Acoustic Delay Lines," Microwave J., 1–5 (March 1970).
- A. N. Broers, "Selective Ion Beam Etching in the Scanning Electron Microscope," Ph.D. Thesis, Cambridge University, U.K., 1965.
- A. N. Broers, "Micromachining by Sputtering Through a Mask of Contamination Laid Down by an Electron Beam," Proceedings of the 1st International Conference on Electron and Ion Beam Science and Technology, R. Bakish, Ed., John Wiley & Sons, Inc., New York, 1964, pp. 191-204.
- A. N. Broers, W. W. Molzen, J. J. Cuomo, and N. D. Wittels, "Electron Beam Fabrication of 80Å Metal Structures," Appl. Phys. Lett. 29, 596 (1976).
- A. N. Broers and R. B. Laibowitz, "High Resolution Electron Beam Lithography and Applications to Superconducting Devices," Future Trends in Superconductive Electronics, B. S. Deavor, Jr., et al., Eds., American Institute of Physics, New York, 1978, pp. 289-297.
- R. E. Howard, J. D. Jackel, and W. J. Skocpol, "Nanostructures: Fabrication and Applications," *Proceedings of Microcircuit Engineering* 85, North-Holland Publishing Co., Amsterdam, 1985, pp. 3-16.
- W. S. Mackie, W. Patrick, S. P. Beaumont, and C. D. W. Wilkinson, "Fabrication of Sub-0.1 Micron GaAs FET's," Proceedings of Microcircuit Engineering 84, Academic Press, London, 1985, pp. 213-218.
- 14. D. F. Kyser and K. Murata, "Monte Carlo Simulation of Electron Beam Scattering and Energy Loss in Thin Films," Proceedings of the 6th International Conference on Electron and Ion Beam Science and Technology, Electrochemical Society, Princeton, New Jersey, 1974, pp. 205–223.
- A. N. Broers, "Resolution Limits of PMMA Resist for Electron Beam Exposure," J. Electrochem. Soc. 128, 166-170 (1981).
- A. N. Broers, "Factors Affecting Resolution in the SEM," Scanning Electron Microscopy/1969, Proceedings of the 3rd Annual Scanning Electron Microscope Symposium, ITT Research Institute, Chicago, 1970, pp. 1–8.
- S. A. Rishton, S. P. Beaumont, and C. D. W. Wilkinson, "Measurement of the Effect of Secondary Electrons on the Resolution Limit of PMMA," *Proceedings of Microcircuit Engineering* 82, Grenoble, Sitecmo Dieppe, Paris, 1982, p. 341.
- J. J. Ritsko, L. J. Brillson, R. W. Bigelow, and T. J. Fabish, "Electron Energy Loss Spectroscopy and Optical Properties of Polymethyl Methacrylate from 1 to 300 eV," J. Chem. Phys. 69, 3931–3939 (1978).
- T. O. Sedgwick, A. N. Broers, and B. J. Agule, "A Novel Method for the Fabrication of Ultrafine Metal Lines by Electron Beams," J. Electrochem. Soc. 119, 1769-1771 (1972).
- A. N. Broers and T. O. Sedgewick, "Method for Making Device for High Resolution Electron Beam Fabrication," U.S. Patent 3.971,860, 1976.
- R. B. Laibowitz, A. N. Broers, J. T. C. Yeh, and J. M. Viggiano, "Josephson Effect in Nb Nanostructures," *Appl. Phys. Lett.* 35, 891–893 (1979).
- R. Voss, R. B. Laibowitz, and A. N. Broers, "Niobium Nanobridge DC SQUID," Appl. Phys. Lett. 37, 656-658 (1980).

- P. Chaudhari, A. N. Broers, C. C. Chi, R. B. Laibowitz, E. Spiller, and J. Viggiano, "Phase-Slip and Localization Diffusion Lengths in Amorphous W-Re Alloys," *Phys. Rev. Lett.* 45, 930–932 (1980).
- C. P. Umbach, S. Washburn, R. A. Webb, R. Koch, M. Bucci, A. N. Broers, and R. B. Laibowitz, "Observation of h/e Aharonov-Bohm Interference Effects in Sub-Micron Diameter, Normal Metal Rings," J. Vac. Sci. Technol. B 4, 383-385 (1986).
- C. J. Buckley, M. T. Browne, and P. Charalambous, "Contamination Lithography for the Fabrication of Zone Plate X-Ray Lenses," SPIE (Society of Photo-Optical Instrumentation Engineers) Proc. 537, 213 (1985).
- A. N. Broers, J. J. Cuomo, J. Harper, W. Molzen, R. B. Laibowitz, and M. Pomerantz, "High Resolution Electron Beam Fabrication Using a STEM," *Electron Microscopy 1978*, Vol. III, J. M. Sturgess, Ed., Microscopical Society of Canada, Toronto, 1978, pp. 343–354.
- A. N. Broers, J. J. Cuomo, and W. Krakow, "Method for Producing Lithographic Structures Using High Energy Electron Beams," *IBM Tech. Disclosure Bull.* 24, 1534 (1981).
- M. Isaacson and A. Muray, "In Situ Vaporization of Very Low Molecular Weight Resists Using 1/2 nm Diameter Electron Beams," J. Vac. Sci. Technol. 19, 1117-1120 (1981).
- Beams," J. Vac. Sci. Technol. 19, 1117-1120 (1981).
  29. E. Kratschmer and M. Isaacson, "Nanostructure Fabrication in Metals, Insulators and Semiconductors Using Self-Developing Metal Inorganic Resist," J. Vac. Sci. Technol. B 4, 361-364 (1986).
- M. E. Mochel, C. J. Humphreys, J. M. Mochel, and J. A. Eades, "Cutting of 20 Å Holes and Lines in Metal-β-Aluminas," Proceedings of the 41st Annual Meeting of the Electron Microscopy Society of America, San Francisco Press, San Francisco, 1983, pp. 100–101.
- A. N. Broers and M. Pomerantz, "Rapid Writing of Fine Lines in Langmuir-Blodgett Films Using Electron Beams," *Thin Solid Films* 99, 323-329 (1983).
- G. A. C. Jones, S. Blythe, and H. Ahmed, "Direct Fabrication of Nanometer-Scale Structures in Semiconductors with 500 kV Lithography," *Proceedings of Microcircuit Engineering 86*, North-Holland Publishing Company, Amsterdam, 1986, pp. 265-271.

Received December 31, 1987; accepted for publication January 8, 1988

Alec N. Broers Cambridge University, Department of Electrical Engineering, Trumpington Street, Cambridge, United Kingdom CB2 1PZ. Prof. Broers is professor of electrical engineering and head of the electrical engineering division at Cambridge University. He took up his current position in 1984, having spent the previous nineteen years working at IBM on electron microscopy, electron-beam lithography, and integrated circuit fabrication. Prof. Broers was elected an IBM Fellow and held a series of management positions in IBM, including those with responsibility for the photon and electron optics groups at the Yorktown Research Center from 1971 to 1981, semiconductor lithography and process development in IBM's East Fishkill Laboratory, and advanced development at East Fishkill. He was also a member of the IBM Corporate Technical Committee. Prof. Broers' personal research has involved the application of small electron beams (diameters down to 0.3 nm) to microscopical and microfabrication problems. This has led to scanning electron microscopy methods that produce resolution of 1 nm when examining the surface of bulk samples, and to fabrication techniques that produce elecrically testable devices of 10 nm and structures below 2 nm in size. Prof. Broers has published numerous articles on high-resolution lithography and related subjects. He received the American Institute of Physics prize for Industrial Applications of Physics in 1981, and the IEEE Cledo Brunetti Award in 1985 for his work on high-resolution electron-beam lithography. He is a Fellow of the Institute of Electrical Engineers, a Fellow of Engineering, and a Fellow of the Royal Society.